2

Study of Some Key Issues for Applying LES to Real Engineering Problems

Xiaolong Yang
Hunan University
China

1. Introduction

Most of nature and industry flows are turbulence. There are three kinds of numerical simulation methods for turbulent flows (Lesieur 1990; Pope 2000; Sagaut 2000, 2006): direct numerical simulation (DNS), Reynolds-averaged Navier-Stokes equations (RANS) and large eddy simulation (LES). DNS is a straightforward way to simulate turbulent flows. Full Navier-Stokes equations are discretized and solved numerically without any model, empirical parameter or approximation. Theoretically speaking, results of DNS exactly reflect the real flow and the whole range of turbulence scales are computed. With DNS, people can compute and visualize any quantity of interest, including some that are too difficult or impossible to be measured by experiments. But as we all know the computation cost is very high. For high Reynolds number flow, even modern computer technology can not satisfy the computation requirement.

In RANS, the flow quantities are decomposed into two parts: the average or mean term and the fluctuating term by applying Reynolds averaging. The effect of the fluctuating quantities on the mean flow quantities is described by the so called Reynolds stress tensor, which is must be modelled in terms of the mean velocities. Typical models can be grouped loosely into three categories: algebraic models, one-equation models and two-equation models. RANS is simple and robust. It is widely used in engineering problem. The general limitation of RANS is the fact that the model must represent a very wide range of scales. While the small scales tend to be universal, and depend on viscosity, the larger scales depend largely on flow condition and boundaries. So there is no one universal model for all flows. For different flows, the model must be modified to obtain good results. Another issue is that usually a time averaging is adopted in RANS. So RANS has difficult to handle unsteady flows.

In LES, a filter is applied to separate the large scales from small scales. Then only the large, energy carrying scales (or called resolved scales) of turbulence are computed exactly by solving the governing equations. While the small, fluctuating scales are modelled, which is also called subgrid scales (SGS). Compared to RANS, LES has several advantages: 1) LES can capture the large scales directly which are the main energy container of turbulence and response for the momentum and energy transfer. 2) The dissipation of turbulence energy is believed to be done by small scales. Since small scales are thought to be homogenous,

universal, and less affected by flow and boundary conditions, the SGS model can be simple and requires fewer *ad hoc* parameters when it is applied to different flows. This is the big advantage of LES over RANS. That also is the reason why simple Smagrinsky model can obtain reasonable results in different flows. 3) LES can solve the unsteady flow directly. In additional, LES requires much less computation resource when compared to DNS because only large scales are computed.

Although LES has some advantages, for a long time RANS methods were used almost exclusively for the analysis of turbulent flows for practical engineering problems. LES has largely been used to study simple turbulent flows(Mahesh et al 2004; Georgiadis 2008; Bouffanais 2010). The primary reason is the computational cost. Until recently, the field of LES is attracting more and more people's attention. Not only its own scientific researcher who is applying LES to study the turbulence, but more industrial partners and engineers have started implementing LES to study real complex flows. There are two main reasons: 1) the urgent requirements from industry. the characteristics of lots nature or real engineering flows are determined by unsteady large scale motion, such as the external flow around ground vehicle, high attack angle airfoil flow etc. RANS models usually have difficult to handle such flows. But in order to improve the performance of airplane, to reduce the drag and noise around vehicle, we have to investigate such flow in depth. (2) rapid increases in computing power, memory, and storage, plus high efficient and high order computation algorithm. Indeed in the past few years applying LES to real engineering flows has becomes a research *hot spot*, such as LES of airfoil (Mary&Sagaut 2001; Dahlstrom&Davidson 2003; Mellen et al 2003), ground vehicle (McCallen *et al.* 2006; Kitoh *et al.* 2009; Krajnovic&Davidson 2005; Rodi 2006; Tsubokura *et al.* 2009; Minguez *et al.* 2008), combustion and reacting flows (Moin 2002), weather forecasting etc. But the application of LES is still limited. There are some key issues needed to solved before LES can be successfully applied to real engineering turbulence(Georgiadis 2008; Bouffanais 2010), such as the suitable SGS model, the choice of filter, the wall model, the transition model, the effect of numerical errors and the interactions between these issues. However as Bouffanais (Bouffanais 2010) pointed out that despite the numerous challenges still facing LES, one can fairly admit that LES has become one of the most promising and successful methodology available to simulate industrial turbulent flows.

In this chapter, three key issues of LES are discussed briefly: the SGS model, the filter and the numerical errors. First, the SGS model is the most important item in LES and has been extensive studied. There are thousand of different models which have been proposed during the past. But most of them are limited to simple geometry and have difficult to be applied to engineering problems. Right now the most widely used SGS models in complicated turbulence are still the simple Smagrinsky model (Smagorinsky 1963) and the so called the monotone integrated LES (MILES) model. So a simple, robust, efficient and can handling complicated geometry SGS model is what we need. The second problem is the choice of filter. In simple geometry, usually a smooth filter is adopted which is defined continuous in the whole domain. But in complicated geometry, only local discrete filter can be used. Obvious the order of filtering will be decreased. Its effect on SGS model and final simulation result need to be investigated. The third is the numerical errors of different discretization schemes. The effect of numerical errors on LES is a delicate issue and has been ignored for a long time because in simple geometry very high order can be achieved by pseudo-spectral mothod or other algorithm. But for complex problem, usually only second order can be achieved. The interaction between numerical scheme and SGS model is complicated. A first extensive

theoretical analysis of numerical errors in LES has been proposed by Ghosal (Ghosal 1996) and later Chow and Moin (Chow and Moin 2003). They believed that 2nd order discretization scheme is not suitable for LES because it introduces errors larger than the SGS term. High order schemes are necessary. By applying the eddy-damped quasi-normal Markovian (EDQNM) theory to LES, a so called dynamic error analysis has been performed by Park and Mahesh (Park and Mahesh 2007) Their results show that low order scheme is acceptable for LES. The study of Yang and Fu (Yang and Fu 2008) show that there are complicated interactions between SGS model and numerical errors. A good SGS model can not only represent the effect of small scales to large scales, but also can dump the unphysical energy introduced by numerical scheme. So by careful designed SGS model, low order discretization scheme can also obtain reasonable result. Fauconnier *et al* (Fauconnier *et al* 2009) also point out that low-order methods may have advantages over high order scheme because the dissipation error of SGS model can cancel part of the numerical errors resulting in a reduction of the total errors on some quantities. Of course the disadvantage is that the accuracy of small scales is not controlled. So the best is high order scheme plus high accurate SGS model.

2. Governing equations and numerical methods

In Large Eddy Simulation (LES) a filtering operation is applied to separate the large scales from the small scales (Leonard 1974). In general, a filtered variable can be written as

$$\overline{f}(x) = \int_D f(x')G(x,x';\overline{\Delta})dx' \tag{2.1}$$

where G is the filter kernel and D is the filtering domain. The filter is characterized by a filter width $\overline{\Delta}$. The corresponding wave number $k_c = \pi/\overline{\Delta}$ is called as the filter cut-off wave number.

For our study, the fluid is assumed to be incompressible; the viscosity is constant; there are no body forces; and the flow is initially homogenous, isotropic, i.e. there are no mean velocity gradients. So the incompressible Navier-Stokes equations after applying a low-pass filter can be written as

$$\frac{\partial \overline{u_i}}{\partial t} + \frac{\partial \overline{u_i}\,\overline{u_j}}{\partial x_j} = -\frac{1}{\rho}\frac{\partial \overline{P}}{\partial x_i} + \frac{\partial}{\partial x_j}\left[\nu\left(\frac{\partial \overline{u_i}}{\partial x_j} + \frac{\partial \overline{u_j}}{\partial x_i}\right)\right] - \frac{\partial \tau_{ij}}{\partial x_j}\,\frac{\partial \overline{u_i}}{\partial x_i}. \tag{2.2}$$

Above equations are also called the incompressible LES equations. The u, P, ρ, ν are the velocity, pressure, density and kinematic viscosity, respectively. τ_{ij} is the subgrid stress (SGS) tensor

$$\tau_{ij} = \overline{u_i u_j} - \overline{u_i}\,\overline{u_j}. \tag{2.3}$$

It represents the effect of the unresolved (small) scales. It is the only unclosed term in the above LES equations (2.2) and should be parameterized in terms of the resolved (large) scales.

In order to isolate other effects, the simplest homogenous, isotropic turbulence is chose as our simulation case. The advantage is that we can obtain the statistical quantities of this turbulence easily in spectral space, such s energy spectrum, total kinetic energy etc. So in

such case it is convenience to write the governing equations in spectral space. Note the continuity equation can be combined with the pressure term through the projecting operation (Lesieur 1990). So the governing equation in spectral space can be simplified as

$$\left(\frac{\partial}{\partial t}+\upsilon k^2\right)\hat{u}_i(\mathbf{k},t)=-P_{im}(\mathbf{k})ik_j\widehat{u_ju}_m(\mathbf{k})\,. \tag{2.4}$$

where '$\wedge$' means the Fourier transform, the tensor $P_{im}(\mathbf{k})=\delta_{im}-k_ik_m/k^2$ is called the projection operator, which ensures the continuity equation automatically satisfied. And the $k=|\mathbf{k}|$.

For spatial discretization, a computation method similar to Rogallo's (Rogallo 1981) is adapted here. For the viscous term in the left hand side of equation (2.4), Rogallo proposed an integrated factor method which can solve it analytically.

$$\frac{\partial}{\partial t}\left[e^{\upsilon k^2 t}\hat{u}_i(\mathbf{k},t)\right]=-e^{\upsilon k^2 t}P_{im}(\mathbf{k})N_m(\mathbf{k})\,. \tag{2.5}$$

So the only term needed to be discretized is the nonlinear term in the right hand side, $N_m(\mathbf{k})=ik_j\widehat{u_ju}_m(\mathbf{k})$, which usually is solved by high order spectral scheme. But for engineering problem, spectral method is not available at most cases. Finite difference scheme or finite volume scheme is used instead. Among them, Padé compact scheme is widely adapted due to its flexibility in handling complex geometry and to obtaining high order. For one dimensional derivative, the Padé scheme proposed by Lele (Lele 1992) can be expressed as

$$\alpha f'_{i-1}+f'_i+\alpha f'_{i+1}=a\frac{f_{i+1}-f_{i-1}}{2\Delta}+b\frac{f_{i+2}-f_{i-2}}{4\Delta}\,. \tag{2.6}$$

Different coefficient defines different order of compact scheme. The highest order is 6th for 3 point stencil. The parameters of Lele (Lele 1992) are shown in Table 2.1.

Scheme	α	a	b	Order
Padé2	0	1	0	2
Padé4	1/4	3/2	0	4
Padé6	1/3	14/9	1/9	6

Table 2.1. Parameters for Padé compact scheme.

For the temporal advancement of the nonlinear term, an explicit second-order Runge-Kutta scheme, also known as predictor-corrector scheme, is used. It's simple and efficient. Briefly, equation (2.5) with only nonlinear term on the right hand side can be seen as the following form

$$\frac{\partial}{\partial t}u=N \tag{2.7}$$

where N represents the nonlinear term. By applying second-order R-K scheme to above equations, we get

$$\frac{u^* - u^n}{\Delta t} = N^n \tag{2.8}$$

$$\frac{u^{n+1} - u^n}{\Delta t} = \frac{1}{2}\left(N^n + N^*\right) \tag{2.9}$$

where n and n+1 represent the different time steps, and * represent the middle step variable. Eq. (2.8) is also called the predictor step and Eq. (2.9) is called the corrector step.

3. SGS model

In LES, only the large, energy carrying scales of turbulence are computed exactly. Specify in LES equation (2.2), the large scales are the filtered velocities, $\overline{u}_i$, which are also called the resolved scales. The small ones, u_i' , (unresolved, or subgrid scales) have been removed from the equation and needed to be modelled, i.e. τ_{ij} in equation (2.2).

The SGS model is the key issue in LES. Since only large scales are resolved in LES, the energy transfer from large scales to small scales is cut off. The energy will accumulate at the cut-off wave number and lead to the unphysical solution. So the main role of SGS model is to provide necessary small scales dissipation and thus remove the accumulated energy. There are many different approaches for the modelling of the SGS stress tensor. Traditionally they are divided into three main categories: eddy viscosity models, similarity models and mixed models. Discussion of standard LES models can be found in some review paper, such as Piomelli (Piomelli 1999), Mathew (Mathew 2010) etc. Below we only discuss the eddy viscosity model briefly.

The eddy viscosity models assume:

$$\tau_{ij} = \overline{u_i u_j} - \overline{u}_i \overline{u}_j = -2\upsilon_t \overline{S}_{ij} + 1/3\,\delta_{ij}\tau_{kk} \tag{3.1}$$

which relate the SGS stresses to the large scale strain-rate tensor S_{ij} , where S_{ij} is

$$s_{ij} = \frac{1}{2}\left(\frac{\partial u_i}{\partial x_j} + \frac{\partial u_j}{\partial x_i}\right) \tag{3.2}$$

and ν_t is the eddy viscosity. Like RANS, equation (3.1) was developed by analogizing to the molecular viscosity. So different eddy viscosity models are actually different methods to calculate the ν_t.

The Smagorinsky model (Smagorinsky 1963) is perhaps the most successful SGS eddy viscosity models, which takes eddy viscosity proportional to the product of Δ^2 and $|\overline{s}|$,

$$\nu_t = \left(C_s\Delta\right)^2 |\overline{s}| \tag{3.3}$$

where C_s is called the Smagorinsky constant, Δ is the grid size and $|\overline{s}| = \left(2\overline{s}_{ij}\overline{s}_{ij}\right)^{1/2}$ is the magnitude of the strain-rate tensor. By choosing different C_s for various flows, Smagorinsky model has been used with considerable success. For isotropic decaying turbulence, the value of the Smagorinsky constant is taken to be around 0.18~0.23 (Lilly (Lilly 1996)), but in shear flow or near boundaries, C_s must be decreased and values 0.06~0.1 are preferred (Piomelli *et al.* (Piomelli *et al.*1988)).

Smagorinsky model can properly account for the global energy transfer. It is simple and robust, which make it the most widely used SGS model. But the modeled SGS quantities correlate poorly with the actual SGS quantities obtained from DNS. Moreover it is an absolutely dissipative model and tends to overestimate the SGS dissipation. It only allows one way energy flux, i.e. from large scales to small ones, and it fails to predict the inverse energy transfer from the subgrid scales to the resolved scales (backscatter) which is found in most flows. Many *ad hoc* corrections and variation of eddy viscosity models are proposed to solve the difficulties mentioned above. Among them the dynamic model of Germano *et al.* (Germano *et al.*1991) and its variations are the most attractive ones. The dynamic model calculates the eddy viscosity dynamically and obtains good results in different turbulence. But it still has some problems when applied to complex engineering flows.

3.1 Velocity Estimation Model (VEM)

To construct a reasonable and reliable SGS model, to properly predict the interactions between large scales and small scales is the key, which means we need to know more detailed information about the nonlinear interactions between large and small scales. Fortunately during the last several years there are many investigations in a variety of turbulent flows, including isotropic and channel flow, at low Reynolds numbers using direct numerical simulation databases and experimental measurements (Zhou 1993; Hartel *et al.* 1994; Domaradzki & Rogallo 1990). Their studies show that the large scales contain enough information. Many of the observed features of the exact SGS interactions can be inferred from the dynamics of the resolved scales alone. Thus it implies a possible way to improving SGS model, i.e. to estimate the small scales from large scales by using the observed properties of the nonlinear interactions. Based on that concept, Domaradzki *et al* (Domaradzki & Saiki 1997; Domaradzki et al 2002) develop the velocity estimation model in both spectral and physical space. Stolz and Adam also proposed similar model called deconvolution model (Stolz 1999).

The velocity estimation model is based on two observations: first, the dynamics of small scales are strongly determined by the large, energy carrying eddies; second, the contribution of small scales to large scales are mostly contained within wavenumbers that are twice that of the cutoff wavenumber, k_c. These two observations rely on the properties of nonlinear interactions in turbulent flows and have been elucidated by a large number of theoretical, numerical and experimental investigations (Zhou 1993; Domaradzki & Rogallo 1990; Domaradzki & Saiki 1997; Domaradzki et al 2002). Basically these studies showed that most of the subgrid scale transfer happens in the range of $0.5k_c \sim k_c$ and is determined by scales in the range of $k_c \sim 2k_c$. This implies that only a limited range of wavenumbers needs to be considered. Especially in VEM the modes beyond $2k_c$ are ignored. With a proper estimation of the velocity field the subgrid scale stress tensor could be determined directly from the resolved scales and provides enough dissipation for LES.

The eddy viscosity models basically try to solve the imaginary υ_t by related to the large scale strain-rate tensor. If we know the full velocity field of the turbulence flow, the τ_{ij} can be calculated directly from the definition equation (2.3) and do not need any assumption. Since the velocity in LES is the filtered velocity, a simple way to recover the full velocity is defiltering, i.e., an inversion of the filtering operation (2.1). Such a procedure is also called deconvolution. But the defiltered velocity does not contain any small scales information.

Domaradzki *et al* (Domaradzki & Saiki 1997; Domaradzki et al 2002) proposed a method to estimate the small scales. This is the basic idea of the velocity estimation model. In order to describe the different velocities, we use u to present the full, unfiltered turbulence velocity; $\overline{u}$ means the filtered velocity; and u' is the small scale velocity. And the relation among them is

$$u = \overline{u} + u' \tag{3.4}$$

VEM contains two steps: First is the defiltering operation, i.e. try to recover the full velocity u from the filtered velocity $\overline{u}$

$$u \approx G^{-1}\overline{u}\,, \tag{3.5}$$

which is inverse operation of (2.1). Bertero and Boccacci (Bertero & Boccacci 1998) give a detailed discussion about it. Since any filtering will loss part of original information, the defiltering can not recover the full velocity according to Riemann–Lebesgue theory. Only some very special filtering function and variables can return to its original state. Most results of defiltering can only be approximate. The velocity u in equation (3.5) actually only contains large scales information, so we denote it by $\tilde{u}^0$. If we using tophat filter and the filtering size is twice as the grid size, then the filtering operation can be expressed as

$$\overline{u} = au_{i-1} + bu_i + cu_{i+1}\,, \tag{3.6}$$

and a, b, c are constants. Then the defiltering operation is

$$a\tilde{u}^0_{i-1} + b\tilde{u}^0_i + c\tilde{u}^0_{i+1} = \overline{u}\,. \tag{3.7}$$

By defiltering, the large scales $\tilde{u}^0$ is closed to the original u, but there is no small scales. If we approximate the u using $\tilde{u}^0$, i.e. let $u \approx \tilde{u}^0$. And then calculate the SGS tensor τ directly from the definition $\tau = \tilde{u}^0\tilde{u}^0 - \tilde{u}^0\ \tilde{u}^0$. Through practice, it is found that if the Reynolds number is not too high, the result is good enough. But if the Re number is high, the error is somehow too large. The information of the small scales is needed. The second step of VEM is to estimate the small scales. For full developed turbulence, the small scales are thought to be homogeneous, so a simplified way to estimate small scales can be described as

$$u' = \theta N'\,. \tag{3.8}$$

where N' is the growth rate of subgrid scales due to the nonlinear interactions among resolved scales and θ is the time scale related to the eddy turn-over time. The detailed description of the full process can be found in paper (Domaradzki & Saiki 1997; Domaradzki et al 2002). Thus the final velocity can be expressed as

$$u \approx \tilde{u} = \tilde{u}^0 + u'\,. \tag{3.9}$$

Correspondingly, the SGS stress tensor is

$$\tau = \overline{\tilde{u}\tilde{u}} - \overline{\tilde{u}}\ \overline{\tilde{u}}\,. \tag{3.10}$$

The energy spectral of full (DNS), filtered, defiltered and estimated velocity are shown in Fig. 3.1

VEM was implemented in both spectral and physical space. It was applied to different flows, such as homogenous tubulence, incompressible channel flow, Rayleigh-Bénard convection flow, and obtained quite good results. But the disadvantage of VEM is that the procedure it uses is quite complicated and need much more CPU time than Smagorinsky model.

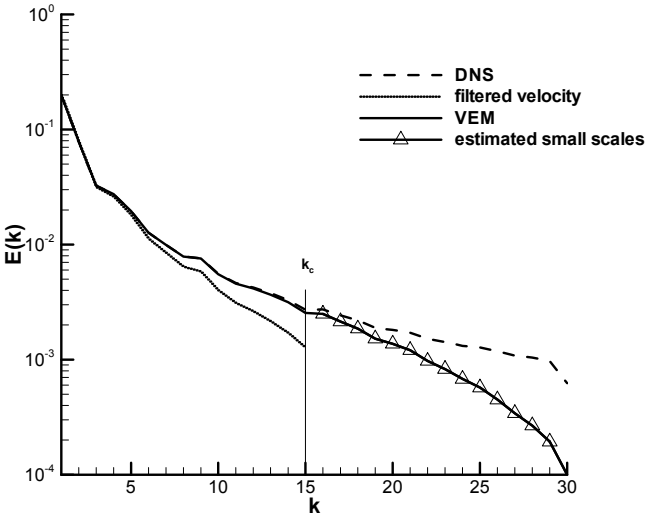

Fig. 3.1. Sketch of energy spectral for full (DNS), filtered, defiltered and estimated velocity.

3.2 Truncated Navier–Stokes (TNS) equations approach

As we can see, the traditional eddy viscosity models use the filtered velocity to calculate τ_{ij}, while the VEM tries to recover the full velocity from the filtered velocity and then use it to calculate τ_{ij}. So one may think: if we can get the full velocity from the experiment data or DNS directly, can we just skip the filtering and defiltering steps? Based on that concept, Domaradzki *et al* (Domaradzki et al 2002; Domaradzki & Yang 2004) developed a new TNS approach from VEM model. TNS uses the full velocity. It actually solves the N-S equations directly instead of LES equations. So it does not have the SGS term. Due to limitation of grid, it is an under-resolved DNS run. According to the energy transfer theory, the energy will accumulate at high modes. A mechanism is needed to provide necessary dissipation to remove the accumulated energy, such as filtering /truncation. A similar model in engine application is the MILES model, which depends on numerical scheme to provide implicit dissipation.

TNS model is still based on the same two observations of energy transfer as VEM. The large energy carrying eddies can determine the dynamics of the small scales; in return, the contribution of the small scales to the large scales are mostly contained within wavenumber range between the cutoff wavenumber, k_c, and $2k_c$. Correspondingly, a scale decomposition is performed in TNS as shown in Fig. 3.2: a range of physical (large) scales up to the traditional LES wave number cutoff k_c, and a range of modeled (SGS or estimated) scales between k_c and $2k_c$. The nonlinear interaction between the low wavenumber modes $k<k_c$ and

the high wavenumber modes $k_c<k<2k_c$ provides a natural dissipation mechanism for the large scales, which also automatically includes the effect of reversing energy (backscatter). The energy accumulated at the subgrid scales $k_c<k<2k_c$ is removed by truncation (filtering) at prescribed time intervals. In the physical space, the explanation for TNS is also straightforward. In the traditional LES, the mesh size is $\Delta_{LES} = \pi/k_c$, denoted as a coarse mesh; while the TNS operates on a fine mesh with the size of $\Delta_{TNS} = \pi/2k_c = \Delta_{LES}/2$. Instead of solving the LES equations on the coarse mesh, full Navier-Stokes equations are solved on the fine mesh with a corresponding filtering operation in physical space. It should be noticed that the filtering time interval plays a critical role in TNS. In order to avoid under-dissipating or over-dissipating, appropriate interval must be carefully chosen (Domaradzki & Yang 2004). The suitable interval depends on the filter type, grid resolution and flow condition.

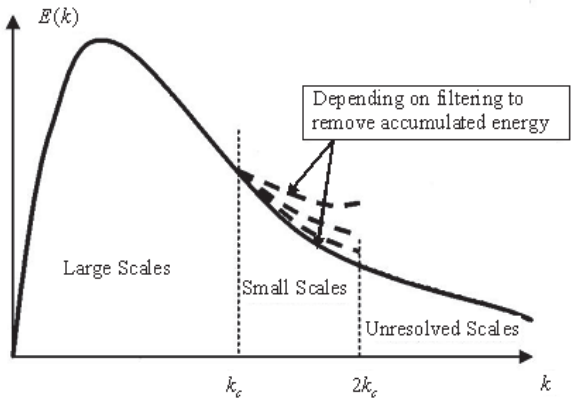

Fig. 3.2. The sketch of TNS in spectral space.

Compared to other LES models, TNS does not have the closure problem because it has no SGS term in the equation. It satisfies the Galilean transformation properties of the Navier-Stokes equations. It is easy to implement with fewer empirical parameters and can be easily extended to other types of turbulence without too much modification. When the explicit filtering is used, the TNS model also shows its advantages over the other models. For instance, as mentioned by Lund (Lund 1997), adaptation of the second explicit filtering leads the SGS term actually to be

$$\tau_{ij} = \overline{u_i u_j} - \overline{\overline{u}_i \overline{u}_j} \ . \tag{3.11}$$

This is not Galilean invariant in most cases. In TNS, this problem is naturally avoided since no such term exists.

TNS was tested in several different turbulent flows. Here only the results of the simplest homogeneous, isotropic decaying turbulence are discussed. For this simple flow there are lot of DNS and experiment data which can be used to test LES model. Here the DNS data of Horiuti (Horiuti 1999) is used, which have a resolution of 256^3. The initial condition for LES is obtained from DNS by truncating the full 256^3 DNS field to 32^3 in spectral space, see Fig.

5.1. Notice the energy at the cutoff k_c=15 may not be small enough compared to the energy peak. Usually for LES models in order to get good results, the energy at cutoff should be two orders of magnitude less than the energy peak. The initial parameters are summarized in Table 3.1

υ	E_0	ε	L	λ	Re_L	Re_λ	t_{ett}
1/720	0.686	0.152	0.51	0.24	245	118	0.68

Table 3.1. Initial parameters.

Fig. 3.3 shows the initial and final energy spectrum for TNS and DNS results. Note that in order to compare the results of other LES models are also presented, including Smagorinsky model and Chollet-Lesieur (C-L) eddy viscosity model (Chollet & Lesieur 1981). The C-L model in spectral space can be expressed as

$$\mu_t(k) = \upsilon^*(k/k_c)\left[E(k_c)/k_c\right]^{1/2}. \tag{3.12}$$

υ^* is the normalized eddy viscosity, which is defined as

$$\upsilon^*(k/k_c) = Ko^{-3/2}\left[0.441 + 15.2\exp(-3.03k_c/k)\right]. \tag{3.13}$$

where *K*o is the Kolmogoroff constant, and is usually set to 1.4.

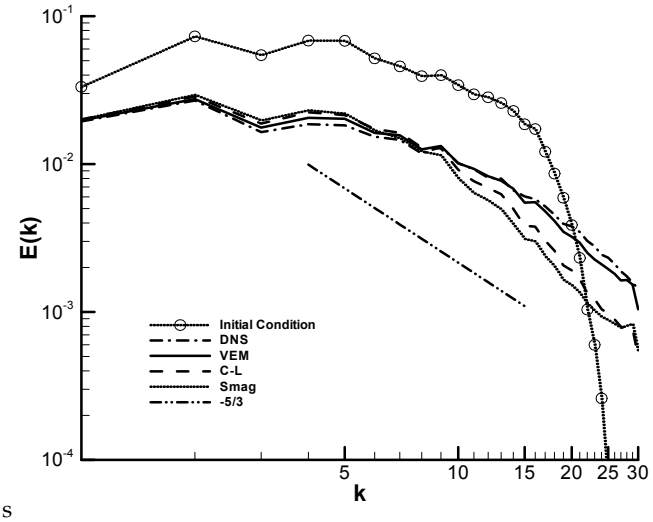

s

Fig. 3.3. Initial and final energy spectrum for DNS, LES and TNS.

As we can see from Fig. 3.3, all models obtain reasonable results compared to DNS, especially at low modes they match each other quite well. However at high modes TNS spectrum matches the result of DNS best, and the $k^{-5/3}$ spectral form is preserved. For Smagrinsky model, as indicated by many studies, the dissipation is overestimated and biggest. C-L shows good results but not as good as TNS. Fig. 3.4 shows the history of

normalized energy decay for all models. Note here we simply divide the energy $E(t)$ by the initial total energy $E(0)$ to get normalized energy. Again TNS gets the best results while the Smagrinsky model shows too much dissipation.

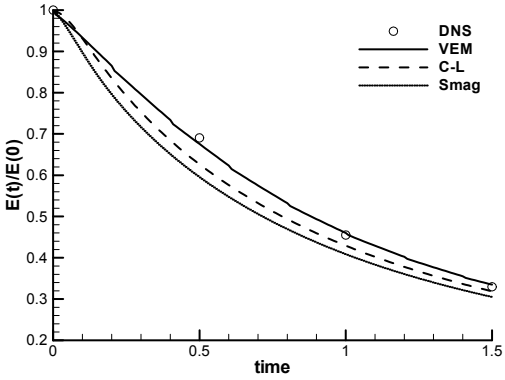

Fig. 3.4. The history of total energy decaying.

4. The choice of filters

The filter shape and filtering width are the two free parameters in LES. Each affects the LES results greatly. Designing suitable filter type and filtering width is important to get reasonable results. In dynamic Smagrinsky model and similarity model, the effect of the filtering width has been studied by Lund (Lund 1997), De Stefano and Vasilyev (De Stefano and Vasilyev 2002) etc. In order to separate these two effects from one another, the present study is focus on the importance of the filter shape.

Theoretically, the filtering operation should be repeated every time step because the nonlinear term continuously generates high frequency modes that need to be dissipated (Lund 1997). Depending on the type of filter, the SGS model should be adjusted in order to represent the dynamics of the unresolved scales correctly. Consequently the nature of the LES solution strongly depends on the filter shape. But for the traditional LES, especially for the eddy viscosity model, there is no explicit filtering process during the calculation in spite of the reasons mentioned above, i.e., the simulation result is independent of the filter. In the conventional practice, the filter has been only used as a concept (Fröhlich & Rodi 2001). The effect of the filter shape on LES is rarely discussed in the literature.

On the other hand, a suitable LES model is needed to test different filters. As just mentioned, most traditional eddy viscosity models do not have explicit filtering in the solution procedure. In the similarity models and the dynamical Smagorinsky model the filtering width of the test (second) filter plays a key role besides the filter shape. A more appropriate LES model, which can directly validate different filters, is therefore required. From section 3.2 we found that the filtering plays a key role in TNS. The dynamics of the large scales and the energy budget strongly depend on the filter shape. It is a very good model to study the filter effect.

There have been many filters proposed in the literatures that can be categorized into two groups: *smooth filters* and *discrete filters*. At the early stage of development, LES was mostly

performed in spectral space in which the filters were defined as continuous in the whole domain. These filters are referred to as smooth filters. The most commonly used ones are the Tophat (box), the Gaussian, and the sharp spectral (Fourier cutoff) filters. Recently, the application of LES to solve real engineering problems in the complex flow has become realistic and, in fact, popular because of the urgent need from the industry. Finite difference scheme instead of pseudo-spectral method is now widely adopted in the numerical approach due to its flexibility in handling complex geometry and obtaining high order schemes (Lele 1992, Visbal & Gaitonde 2002). The finite difference discretization scheme, together with the limited grid resolution, can be seen as an implicit filtering as mentioned by many researchers (De Stefano and Vasilyev2002; Fröhlich & Rodi 2001; Lund 2003; Vasilyev 1998). However this kind of implicit filtering has some problems because of the interactions among the modified terms in the governing equations, the numerical error, and the order of the filter, etc.(Lund 2003; Vasilyev 1998). In order to avoid some of these problems, researchers tend to employ the explicit filtering to exert direct influence on the simulation result. These filters are usually defined on several adjacent points and, hence, denoted as discrete filters thereafter. There are several advantages using explicit filter: First it is easier to control the truncation and aliasing errors by removing the high wave number modes which is beyond the bandwidth allowed by the mesh. Second it can dump the oscillation at high frequency which comes from the numerical discretization scheme, boundary condition, etc. The amplitude of these oscillations usually is comparable to or even larger than that of the small scales after sufficiently long computation time, which tends to contaminate the final result of the simulation. By using the same explicit filter, it also makes the comparison with experiment or DNS data more direct.

4.1 Smooth filters

The smooth filters include the spectral filter, the Gaussian filter, the Tophat filter and those are defined continuously in the whole computation domain. The definitions for the first three can be easily found in some books (Pope 2000). Table 4.1 shows these filter functions in physical and spectral space respectively.

	Spectral space	Physical space
Spectral filter	$\hat{G}(k)=\begin{cases}1, & k\le k_c;\\ 0, & k>k_c\end{cases}$	$G(x)=\dfrac{\sin\left(\pi x/\bar{\Delta}\right)}{\pi x}$
Tophat filter	$\hat{G}(k)=\dfrac{\sin\left(0.5k\bar{\Delta}\right)}{0.5k\bar{\Delta}}$	$G(x)=\begin{cases}\dfrac{1}{\bar{\Delta}}, & \lvert x\rvert\le 0.5\bar{\Delta};\\ 0, & otherwise\end{cases}$
Gaussian filter	$\hat{G}(k)=\exp\left(-\dfrac{k^2\bar{\Delta}^2}{24}\right)$	$G(x)=\sqrt{\dfrac{6}{\pi\bar{\Delta}^2}}\exp\left(-\dfrac{6x^2}{\bar{\Delta}^2}\right)$

Table 4.1. Smooth filters in physical and spectral space $\bar{\Delta}=\pi/k_c$.

The main problem for the Tophat and Gaussian filters is that they remove too much energy of the large scales (Domaradzki et al 2002; Yang & Domaradzki 2004). The spectral filter is thought as the best among these three for LES because it keeps all the large scales while removes all the small scales. However filters defined in the physical space are much flexible

because for most flows transformation to the spectral space is difficult. People are trying to find a filter that is defined in the physical space while has the property of the spectral filter or close to it at the same time.
Actually the filtering operation (2.1)(Leonard 1974) is a linear spatial averaging operation,

$$\overline{f}(x) = L_G\left(f(x)\right) = \int_D G(x,x';\overline{\Delta}) f(x')dx' \tag{4.1}$$

A formal inverse of it in a power series expansion can be expressed as

$$L_G^{-1} = \left(I - \left(I - L_G\right)\right)^{-1} = I + \left(I - L_G\right) + \left(I - L_G\right)^2 + \cdots \tag{4.2}$$

where I is the unity operator. The product of L_G and the first few terms of the above expansion (4.2) actually defines a suitable new filter (Domaradzki et al 2002) (the product of L_G and the full equation (4.2) is equal to I, of course). If only first few terms are selected, the new filter is close to the original filter L_G and the extra computation cost is small. When more terms are selected, the new filter is closer to unity. It has less effect on the large scales but needs much more computation time. Domaradzki *et. al*. (Domaradzki et al 2002) found that the combination of the first three terms in Eq. 4.2 is the best choice and denoted this filter as the physical filter

$$\overline{u} = 3\hat{u}_i - 3\hat{\hat{u}}_i + \hat{\hat{\hat{u}}}_i \tag{4.3}$$

where '^' is the original Tophat filter or Gaussian filter. One thing need to be pointed out is that the results of the Tophat, Gaussian and Physical filters strongly depend on the filter width $\overline{\Delta}$. However the objective of present work is to highlight the importance of the filter shape as mentioned above. In the following analysis, the filter width is fixed for these smooth filters, which is equal to 2 times of grid size Δ.

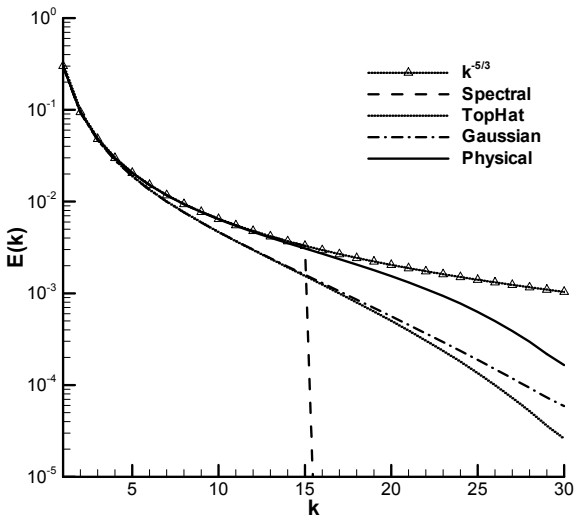

Fig. 4.1. Effect of the smooth filters on the $k^{-5/3}$ spectrum.

The effects of above filters on the $k^{-5/3}$ spectrum are shown in Fig.4.1. As can be seen, the Tophat and Gaussian filters remove too much energy of the low modes. The spectral filter only keeps the large scales. The physical filter strongly damps the small scales while affecting the large scales very little, which make it a good filter for LES.

Beside *a prior* test, the effects of these filters on a real three dimensional LES are also examined. Again the simplest homogeneous, isotropic decaying turbulence is utilized as the test case with two different initial conditions. The first has the initial condition of spectrum $E(k) = Ak^4 \exp\left(-2k^2 / k_p^2\right)$, where $k_\mathbf{p}$ is the peak mode and equals to 4. The grid resolution is 64^3 (In the following, the mesh size is 64^3 for all LES unless further specified). For comparison, the 256^3 DNS result is also included. The final energy spectrum is plotted in Fig. 4.2. It also shows that the Tophat filter removes too much energy (Since the Gaussian filter performs very similarly to the Tophat filter, we did not include it in the figure). The spectral and physical filters show very good agreement with the DNS data.

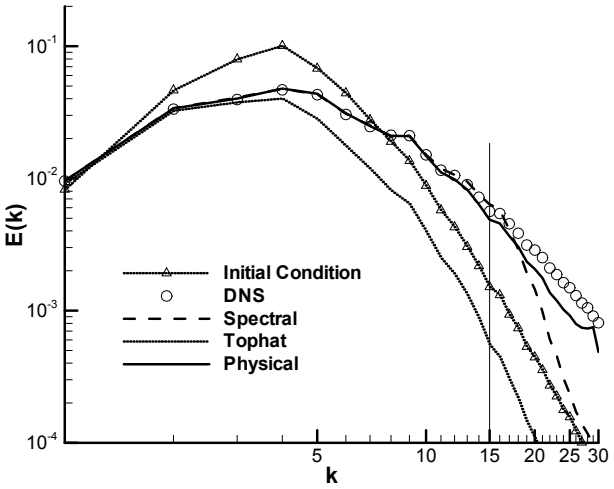

Fig. 4.2. Energy spectrum at final time for LES case 1.

The second case has a more critical initial condition as shown in Fig. 4.3. The initial condition is obtained from the 256^3 DNS data of Horiuti (Horiuti 1999) same as section 3. It is a challenging case for LES because the energy at cut-off mode k_c is not in the inertial range. The Tophat filter shows too much dissipation same as above. However the spectral filter delivers some undesirable behaviors this time. By removing all the small scales, it also shut down the energy transfer from the large to small scales completely. It will take some time for LES to rebuild the nonlinear interactions between the large and small scales, which leads to insufficient dissipation. Thus, the energy accumulates near the cutoff wavenumber as shown in Fig. 4.3. The physical filter provides the best result compared to the DNS data as also observed in paper ((Domaradzki et al 2002; Yang & Domaradzki 2004). The main reason is that the physical filter keeps a small part of the small scales which facilitates the energy transfer. Since this initial condition is a better case to test filters, we only run LES with case two in the following discussion.

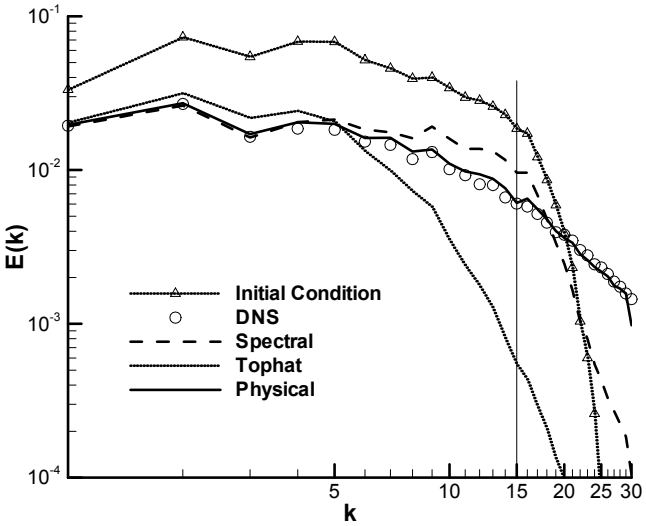

Fig. 4.3. Energy spectrum at final time for LES case 2.

The history of total kinetic energy decay for the smooth filters is plotted in Fig. 4.4. Corresponding to Fig. 4.3, the physical filter obtains better result compared to DNS. Since the spectral filter does not provide sufficient dissipation as shown in Fig. 4.3, its total energy is the biggest among all the results. The Tophat filter removes a part of large-scale energy each time when the filtering operation is applied. That is why the total energy jumps downwards periodically.

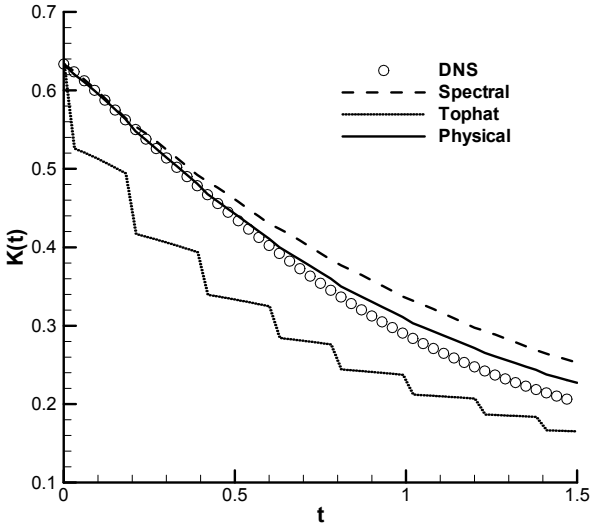

Fig. 4.4. The decay of the total kinetic energy for the smooth filters.

The effect of different grid resolutions is also investigated. The result of LES with grid 32^3 is shown in Fig4.5 and the result for 128^3 is plotted in Fig. 4.6. The behaviors of these smooth filters in coarse mesh (32^3) are almost the same as those in grid 64^3. Physical filter still gets the best results. For the fine mesh (128^3), all filters obtain good result except that the Tophat filter still dissipates a little more. The effect of the SGS model becomes small when the grid resolution increases, which is well known.

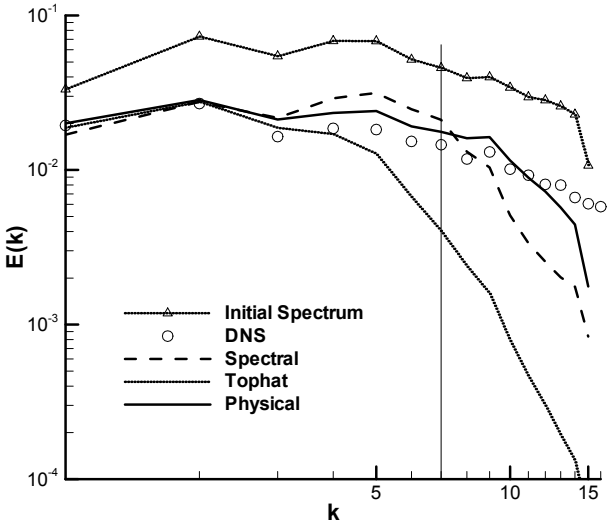

Fig. 4.5. Energy spectrum at final time for the smooth filters with grid 32^3.

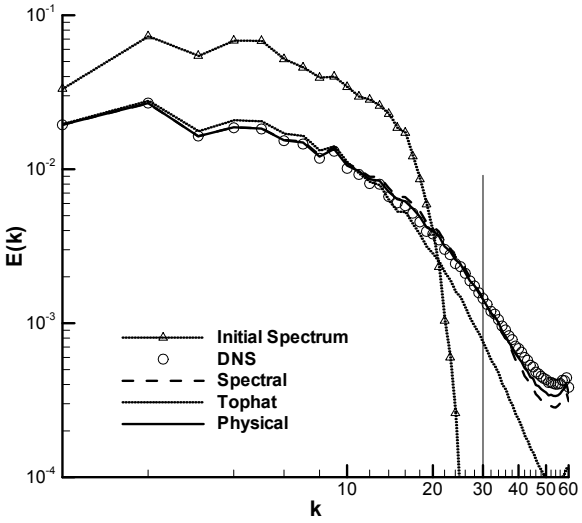

Fig. 4.6. Energy spectrum at final time for the smooth filters with grid 128^3.

4.2 Discrete filters

In order to handle complex geometry, finite difference scheme is widely used instead of the spectral method. The solution is available only on a set of discrete grid points. At most time, the filter for the whole domain does not exist due to the inhomogeneous and boundary condition. The discrete filters, including the discrete Tophat filter, the Padé filter (Visbal & Gaitonde 2002) and the filter series proposed by Vasilyev *et al.* (Vasilyev *et al.* 1998) are utilized rather than the spectral smooth filters

The main problem of the discrete filter is the commutation error between differentiation and filtering operation. Fortunately Vasilyev *et al.* (Vasilyev *et al.* 1998) gave out a solution which can control the commutation error to any specified order. Another problem is that if the order of the filter is too low, the error introduced by filtering may become larger than the magnitude of SGS term. Hence for traditional LES, the filter order is usually required to be higher than that of SGS term. But the filtering operation in TNS only acts as a dissipation source. The numerical error can be included into it as part of the dissipation. Low order filters can also obtain good results. It is similar to the strategy used by Mathew *et al.* (Mathew *et al.* 2003).

A one-dimensional filter given by Vasilyev *et al.* (Vasilyev *et al.* 1998) is defined as:

$$\overline{f}_j = \sum_{l=-K}^{L} w_l f_{j+l} \tag{4.4}$$

In order to control the commutation error to a specified order, the filter is required to have a different number of vanishing moments. Correspondingly, the weight factors w_i should satisfy a set of constrains. These filters are referred as V-filters in the following analysis.

Case	w_{-3}	w_{-2}	w_{-1}	w_0	w_1	w_2	w_3	w_4	w_5
1			1/4	1/2	1/4				
3			1/8	5/8	3/8	-1/8			
6		-1/16	1/4	5/8	1/4	-1/16			
7				31/32	5/32	-5/16	5/16	-5/32	1/32
9		-1/32	5/32	11/16	5/16	-5/32	1/32		
10	1/64	-3/32	15/64	11/16	15/64	-3/32	1/64		

Table 4.2. The weight parameters of the V-filters.

Several sets of weights for the V-filters are given in Table 4.2 which is similar to the Table 1 in Vasilyev *et al*'s paper (Vasilyev *et al.* 1998). The equation (4.4) defines a symmetric (center) scheme if K equals to L. The case 1, 6 and 10 are symmetric and have a commutation error of order 2, 4, 6 respectively. In order to handle boundary points, Vasilyev *et al* also proposed several asymmetric filters, i.e., K and L is different. For high asymmetric V-filters, such as the one side filter - case 7, it is found that too much unphysical energy is introduced to the high modes as also mentioned by Vasilyev *et al* (Vasilyev *et al.* 1998). This property is not desirable for TNS because it will lead to unphysical solution. Thus high asymmetric filters (case 2, 4 5, 7, 8) are not included in the following analysis. Only case 3 and 9 (whose order are 3 and 5 respectively) are tested as well as the symmetric ones.

Fig. 4.7 presents the filtering results of different V-filters applied to the $k^{-5/3}$ spectrum. For comparison, the result of the smooth physical filter is also included. Case 1 in fact is a discrete version of the Tophat filter using trapezoidal rule. Similar to the smooth one, it

removes too much energy of the large scales. It is interesting that the asymmetric filters like case 3 and 9 keep more energy than the symmetric ones (case 6 and 10). Note case 3 and case 6 still remove a small part of the large-scale energy. While case 7 introduces too much energy at high wavenumber modes which will lead to an unphysical solution in a real LES run.

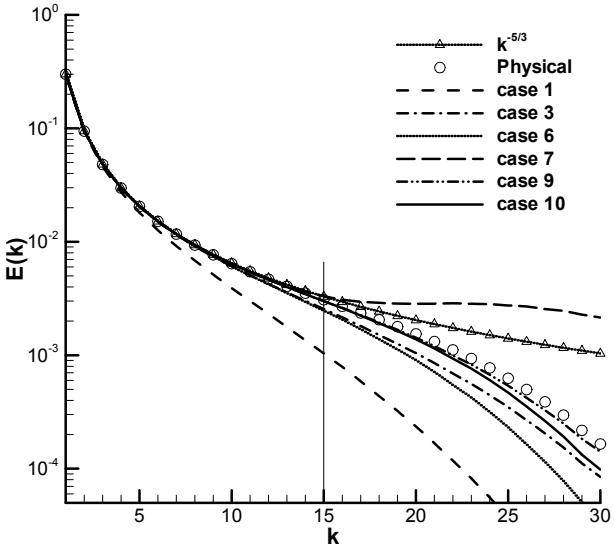

Fig. 4.7. Effect of the V-filters on the $k^{-5/3}$ spectrum.

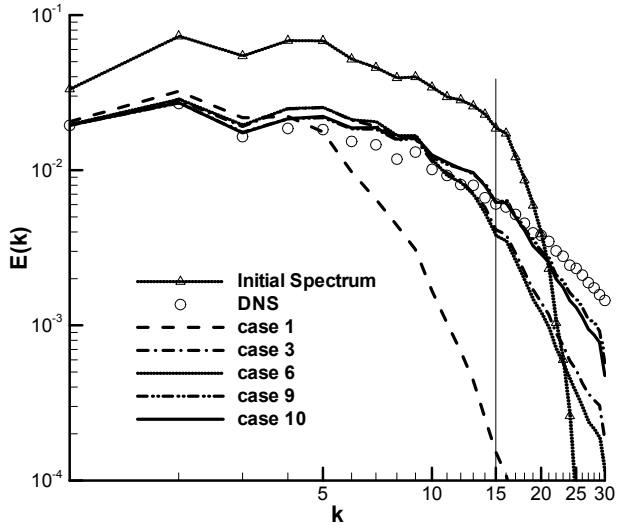

Fig. 4.8. Energy spectrum at final time for the V-filters.

Fig.4.8 shows the final energy spectrum of the V-filters in the same homogeneous run as Fig.4.3. As expected, case 1 dissipates too much energy. High order filters obtains better results. Corresponding to Fig.4.7, the result of the low order asymmetric filter case 3 (3rd order) is a little better than that of the high order symmetric filter case 6 (4th order). And the behaviors of case9 and case 10 are very similar. The reason is still attributed to the fact that a small amount of energy is introduced at high modes for the asymmetric filters. The decay of the total energy is plotted in Fig.4.9. Except case 1, all other cases show good agreement with the filtered DNS data. But there are small jumps for low order filters (case 3 and case 6) because of the undesirable effect to the large scales as shown in Fig.4.7. The effects of grid resolutions on V-filters are similar to the smooth ones, which are not included here.

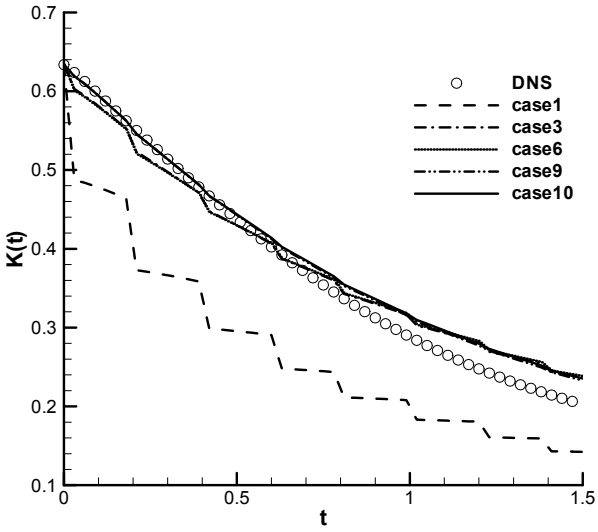

Fig. 4.9. The decay of the total kinetic energy for the V-filters.

Another series of discrete filters is the Padé filters. The Padé compact difference scheme can be regarded as an implicit filter (Visbal & Gaitonde 2002; Vasilyev et al 1998). Based on that, a set of Padé explicit filters is proposed by Visbal and Gaitonde (Visbal & Gaitonde 2002). For a variable *f*, the filtered value can be expressed as:

$$\alpha_f \overline{f}_{i-1} + \overline{f}_i + \alpha_f \overline{f}_{i+1} = \sum_{n=0}^{N} \frac{a_n}{2} \left(f_{i+n} + f_{i-n} \right) \tag{4.5}$$

where α_f is an adjustable parameters between (-0.5, 0.5) and high value of α_f means a less dissipative filter. N is the order of filter scheme, 2N+1 points give a 2N order filter. The coefficients a_n are listed in Table 4.3.

The filtering results of the $k^{-5/3}$ spectrum using different Padé filters are shown in Fig. 4.10. The smooth physical filter is also included as a benchmark. The 2nd order filter removes a small amount of the energy of the low modes, which may have undesirable effect on LES because of the unnecessary dissipation. The 4th order and above have little effect on the

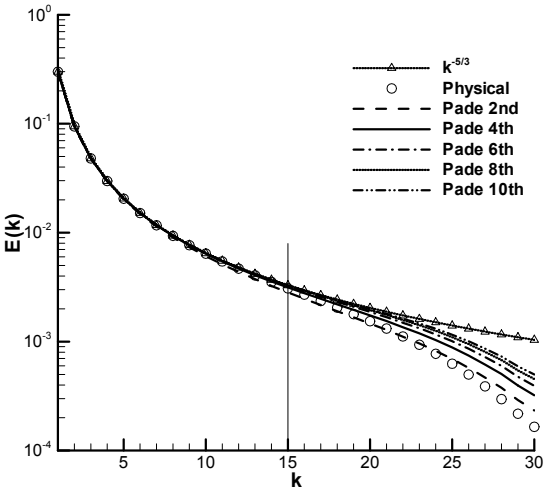

Fig. 4.10. Effect of the V-filters on the $k^{-5/3}$ spectrum.

Scheme	a_0	a_1	a_2	a_3	a_4	a_5
F2	$\frac{1}{2}+a_f$	$\frac{1}{2}+a_f$				
F4	$\frac{5}{8}+\frac{3}{4}a_f$	$\frac{1}{2}+a_f$	$-\frac{1}{8}+\frac{1}{4}a_f$			
F6	$\frac{11}{16}+\frac{5}{8}a_f$	$\frac{15}{32}+\frac{17}{16}a_f$	$-\frac{3}{16}+\frac{3}{8}a_f$	$\frac{1}{32}-\frac{a_f}{16}$		
F8	$\frac{93+70a_f}{128}$	$\frac{7+18a_f}{16}$	$\frac{-7+14a_f}{32}$	$\frac{1}{16}-\frac{a_f}{8}$	$\frac{-1}{128}+\frac{a_f}{64}$	
F10	$\frac{193+126a_f}{256}$	$\frac{105+302a_f}{256}$	$\frac{15(-1+2a_f)}{64}$	$\frac{45(1-2a_f)}{512}$	$\frac{5(-1+2a_f)}{256}$	$\frac{1-2a_f}{512}$

Table 4.3. The Coefficients of the Padé filters.

large scales. But higher the order is, the Padé filter tends to keep more small scales compared to the physical filter. In turn it may not provide enough dissipation for TNS.

The final energy spectra of the LES run with the Padé filters are plotted in Fig. 4.11 and the time evolutions of the total energy are shown in Fig. 4.12. Corresponding to Fig.4.10 the 2nd order filter overestimates the dissipation and subsequently provides the worst results among these runs. The 4th order and above show very good results as compared to the DNS data. However the 6th order and above filters keep more small-scale energy than DNS which may imply them do not provide enough dissipation.

From above results, it is found that the Padé filters show better results than the V-filters. It could be attributed to the fact that the Padé filters consider the effects of adjacent points. On the other hand, the calculation of the V-filters is much simple and straightforward. For the Padé filters we need to solve a tri-diagonal system. It is time consuming and may be

infeasible for the inhomogeneous case. In the Section 4.1 the physical filter shows very good property but it is a smooth filter. So we modified it into a discrete version using the V-filters, i.e. in equation 4.3 we use the V-filters instead of the Tophat filter. Hereafter we denote it as PV-filter.

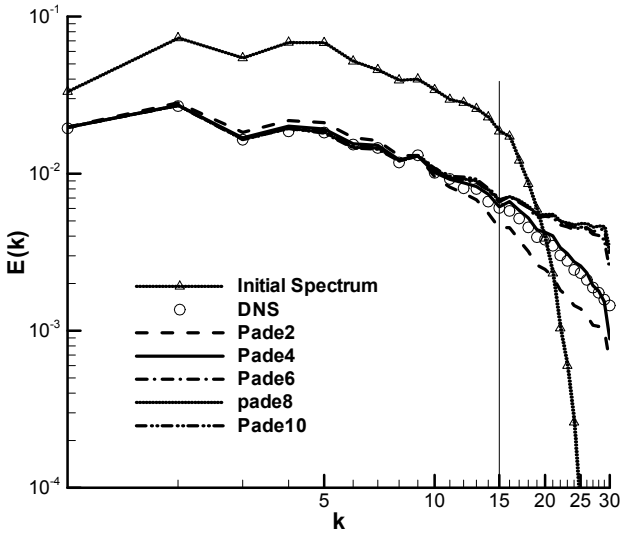

Fig. 4.11. Energy spectrum at final time for the Padé filters.

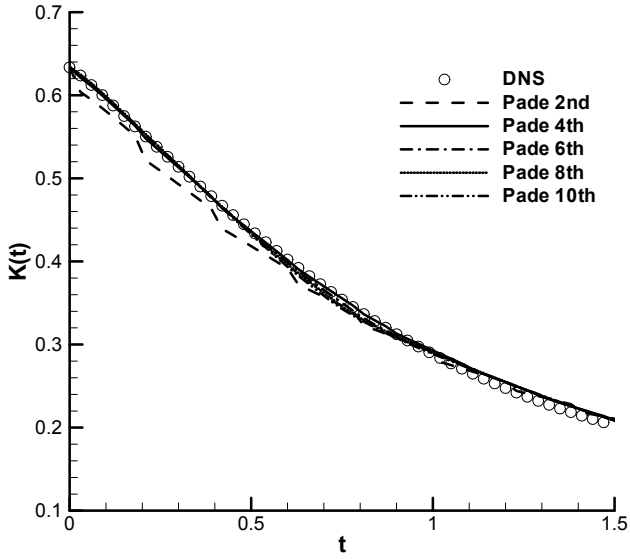

Fig. 4.12. The decay of the total kinetic energy for the Padé filters.

The results of a priori test and the LES run of the PV-filters are shown in Fig. 4.13, Fig. 4.14 and Fig. 4.15 respectively. For comparison, we also include the result of the original case 1 of the V-filter (V-case1) in Fig.4.13. It shows that the result of the 2nd order PV-case1 is improved significantly as compared to V-case1. As mentioned before V-case1 is actually a discrete version of the Tophat filter. Therefore the PV-case1 is a discrete version of the smooth physical filter. Since the result of smooth physical filter is much better than that of the Tophat filter as shown in Fig.4.1, it is no wonder that the PV-case1 is better than the V-case1. However, by comparing Fig.4.14 and Fig.4.3, it was found the results of this discrete version (PV-case1) are not as good as those of the smooth physical filter for a real LES run. Similar to Fig.4.7, the asymmetric filters (PV-case3 and PV-case9) show good behavior in Fig.4.13, keeping more energy than the symmetric ones (PV-case6 and PV-case10). But it was also found that small amount of nonphysical energy is introduced near the cutoff wavenumber. Correspondingly the behaviors of these asymmetric filters in a real LES run are not good as shown in Fig.4.14 and Fig.4.15 (PV-case3 is not shown in Fig.4.14 because the energy spectrum becomes so large that it is out of the scope range). The results of high order symmetric PV-filters are also improved compared to the original V-filters, but not too much.

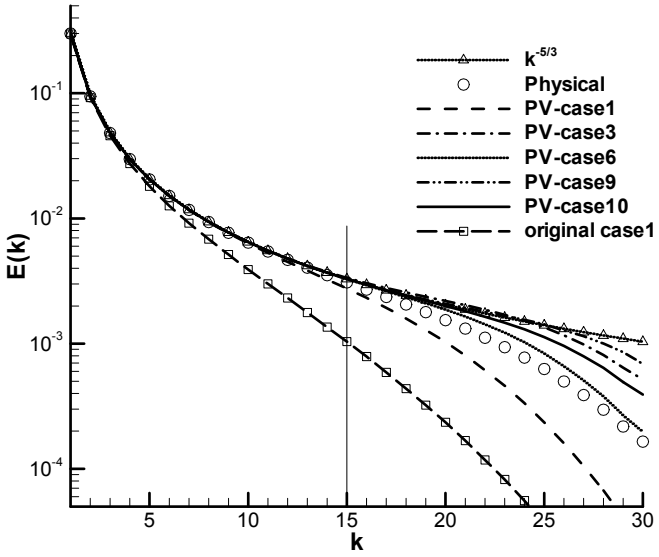

Fig. 4.13. Effect of the PV-filters on the $k^{-5/3}$ spectrum.

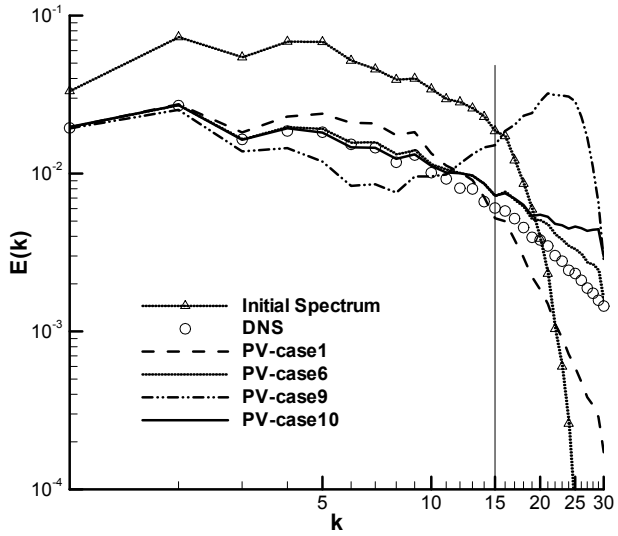

Fig. 4.14. Energy spectrum at final time for the PV-filters.

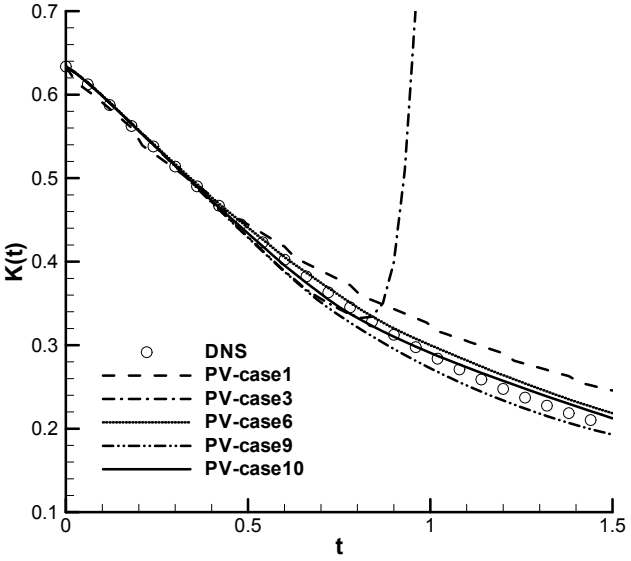

Fig. 4.15. The decay of the total kinetic energy for the PV-filters.

5. The effects of numerical errors on TNS

For DNS, the numerical errors mainly are aliasing and truncation errors (Chow 2003). As for LES, the small scales must be modelled because of the limited grid resolution which can not

resolve all the scales. Therefore LES has an additional source of error comes from the SGS models. In general, it is required that all the source of errors can not overwhelm the contribution of SGS model in LES (Ghosal 1996; Chow 2003). In addition, unlike DNS the cut-off mode in LES is still energetic. As a result, LES is more sensitive to numerical errors. The numerical errors must be well controlled.

Note the numerical error in this section refers to aliasing and truncation errors introduced by spatial numerical scheme. Usually time discretization also introduces some computational errors (He et al 2004). Guo-Wei He etc studied the time correlation of several SGS model on LES (He et al 2004). Here we only focus on the spatial discretization error. In addition, the effect of the floating error of the computer is assumed to be small and ignored thereafter.

5.1 DNS results

We conduct DNS run at first in order to avoid the effect of SGS model. Also DNS data can provide benchmark for LES. The initial condition is the homogenous isotropic turbulence same as section 3 and 4. The grid resolution is 128×128×128 which is found fine enough to resolve the large scales for this simple flow. At Fig.1 the DNS results of 128^3 and 256^3 grid are compared. It is clear shows that they have a very good match for low wavenumber modes. In order to save computation time, only 128^3 runs are carried out thereafter.

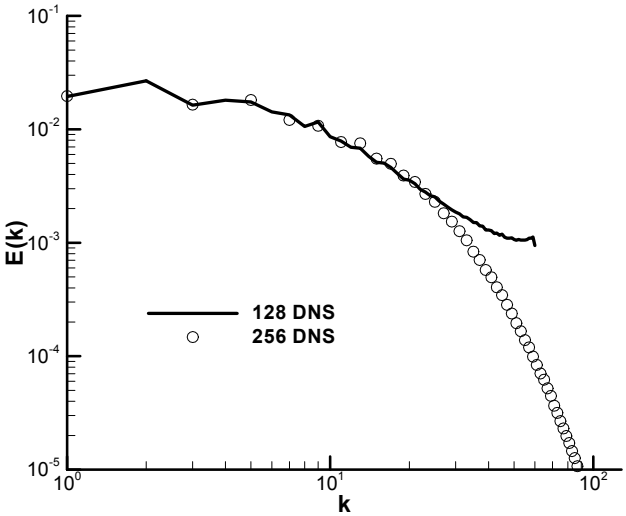

Fig. 5.1. The result of 128^3 DNS compared with 256^3.

As mentioned above, DNS only suffers from aliasing and discretization errors that depend on the numerical scheme used. When spectral method is used, the discretization errors is very small. So the numerical error is dominated by aliasing error. The main reason for aliasing error arising is that the gird resolution is limited. The modes beyond the grid cut-off wavenumber are incorrectly 'aliased' to wavenumbers that are resolved. Usually the contribution of aliasing errors is largest at the highest wavenumbers where any energy above the wavenumber cutoff incorrectly adds on the resolved spectrum. Without control,

aliasing errors destroy the energy conservation and cause the solution to departure from physical solution. Usually a random shift technology is used to eliminate aliasing error. In order to identify the importance of aliasing error, we run two DNS: one uses anti-aliasing technology (the result marked as Dealiased) and the other one does not (the result denoted by Aliased). The simulation results are shown in Fig. 5.1. In Fig. 5.1a the energy spectrum at t=1 (the upper line) and t=3 (the lower line) are shown. And Fig. 5.1b gives the relative value of aliasing error, which is calculated as

$$\sigma(k) = \left(E(k)_{dealias} - E(k)_{alias}\right) / E(k)_{dealias} \tag{5.1}$$

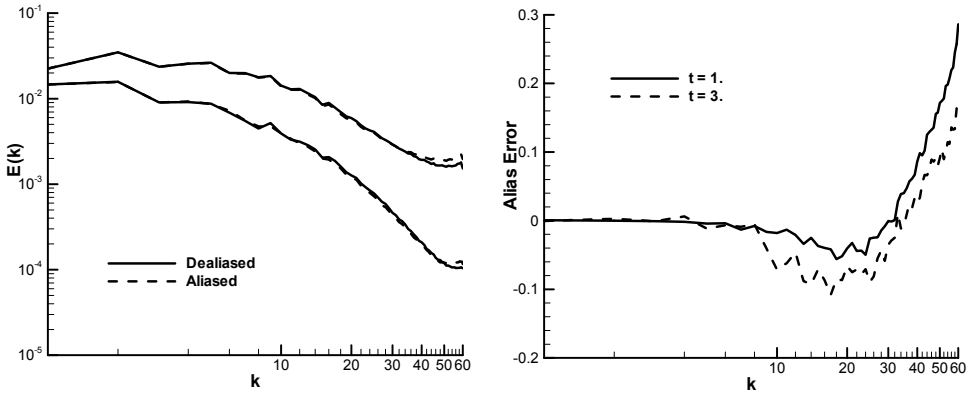

(a) (b)

Fig. 5.2. The aliasing errors for DNS using spectral method.

As we can see, the aliasing error is relatively small for DNS with spectral method. The largest error happens at high modes, which is consistent with the analysis of Park and Mahesh (Park & Mahesh 2007). The aliasing error can contaminate the low modes gradually with time evolution, as shown in Fig.5.1, but it is still very small.

For complex engineering problem, the spectral method is no longer suitable. Finite difference scheme or finite volume scheme is used instead. Same as section 4, the Padé compact scheme is used here. In order to examine the truncation error of different order of Padé scheme, one common used technology is to analysis the modified wavenumber in spectral space (Lele 1992). Similar to aliasing error, Padé scheme has little effect on low modes. The error is highest near the cut-off wavenumber. With higher order, the error is smaller and the result is more close to spectral method.

In order to isolate the discretization error, here we only apply the Padé scheme to the nonlinear term, which is similar to the way used by Kravchenko and Moin (Kravchenko & Moin 1997). The reason is that nonlinear term has important impact on SGS term. Also nonlinear term is a key factor which affects the stability of computation.

In Fig. 5.3 we compare the energy spectrum at different time for spectral method and different order Padé schemes. While the time evolution of total kinetic energy is shown in Fig. 5.4. As we can see, high order scheme, 6th order Padé scheme compares well with spectral method at all time. But for 4th order Padé scheme, at the initial stage (t=1), it

compares well with spectral method at low modes, but shows some difference at high modes. The nonphysical energy introduced by discretization error accumulates at high modes and affects low modes gradually with time developing (t=3)

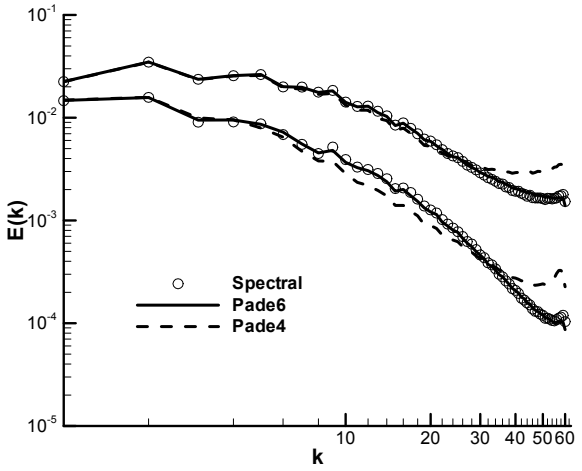

Fig. 5.3. The energy spectrum for DNS using different discretization schemes at t=1 and t=3 (from above to low).

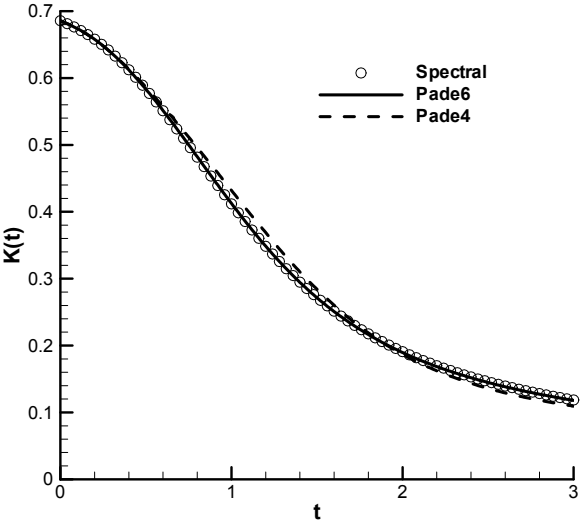

Fig. 5.4. The time evolution of total kinetic energy for DNS using different discretization schemes.

Note that 2nd order Padé scheme actually is the 2nd order center difference scheme. It is well known that it has the problem of even-odd oscillation which will leads to the

computation diverging. We observe the same problem here. Usually an artificial viscosity is needed to dump the oscillation, which is beyond the research scope of this article. In Fig.5.5 the energy spectrum before computation fail is shown. It is clear seen that the nonphysical energy accumulates quickly at high modes which lead to the computation divergence. Park and Mahesh (Park & Mahesh 2007) gave a detail description about this problem. Interested reader should refer to their paper.

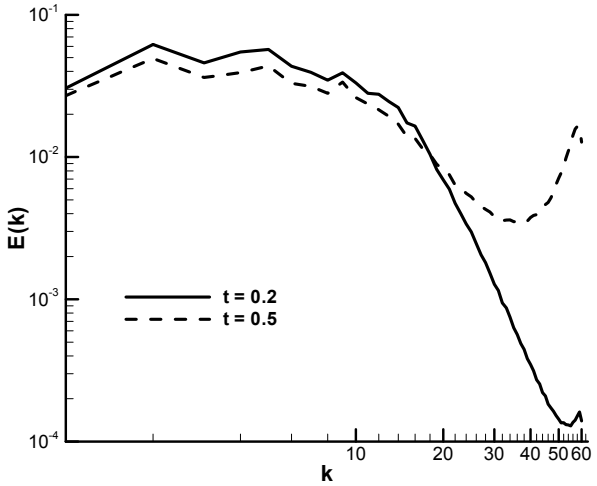

Fig. 5.5. The time evolution of energy spectrum for DNS using 2nd order Padé scheme.

The results for Padé schemes shown in Fig. 5.3 actually contain all the numerical errors, i.e. discretization and aliasing errors. Unlike spectral method, many researches thought that finite difference scheme can automatically decrease the aliasing error and therefore no anti-aliasing method is needed. Since the result of 6th order Padé scheme is the closest one to the spectral method, here we also apply the same anti-aliasing technology as used in spectral method to 6th order Padé scheme (denoted by Dealiased). The new result is then compared with the original one as shown in Fig. 5.6. Compared to spectral method, the magnitude of aliasing error does decrease. Note that actually it is very hard to isolate aliasing error from discretization error. The aliasing error shown above is not the actual aliasing error for 6th order Padé scheme. But anyway we can use that technology to determine the relative importance of aliasing error.
In general, the aliasing error in DNS can be well controlled. The main error is the truncation error of discretization scheme. Low order scheme is not suitable for simulation in some cases.

5.2 LES results

For the same simulations above, we also run the LES. The mesh size is 64×64×64. Spatial discretization adapts the same spectral and Padé compact schemes as in DNS. Note that LES has additional numerical error source which comes from the SGS model besides the aliasing error and discretization error for DNS. Again TNS approach is used to modelling the small scales. TNS model depends on periodic filtering to remove high modes energy. There are

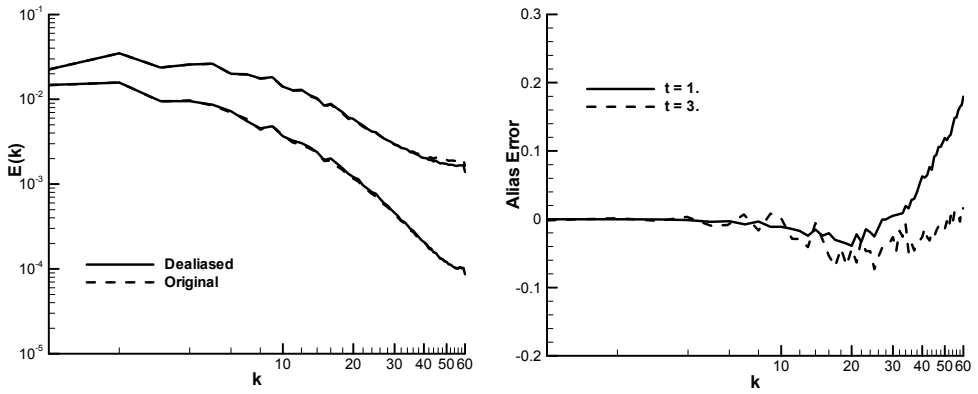

(a) (b)

Fig. 5.6. The aliasing error for DNS using 6th order Padé scheme.

many filters available as mentioned in section 4. Because we pay more attention to the possibility of applying LES to real engineering problem, only discrete filters are adapted here. Since Padé discrete filters show good results in section 4, we only focus on them to simply the research. Note that different order of Padé filter means the error introduced by SGS model is different.

In Fig. 5.7a, b, c, d it shows the final energy spectrum for spectral method and different Padé compact schemes (marked with 'd') combined with TNS model using different order Padé discrete filters (denoted as 'f'), i.e. 'd6f4' means 6th order Padé compact scheme and 4th order filter. As we can see, TNS model plays a key role in the simulations. Low order filter provides too much dissipation and performs poorly for all discretization schemes. High order filter (4th order and above) obtains good results compared with DNS. However higher the filter order is, it keeps more high modes energy and thus dissipates less. In return it decreases the performance of LES. TNS model with 4th order filter provides the best results.

Compared to DNS, LES is not so sensitive to the order of the discretization scheme. Even 2nd order scheme can obtain reasonable results. The result is not as good as of high order scheme though, but much better than of DNS which diverges when using 2nd order scheme. The reason is that the discretization and aliasing errors cause the energy to accumulate at high modes; while TNS model removes high modes energy through filtering. The dissipation provided by SGS model dumps the unphysical energy increment. This result may help explain why low order scheme can obtain good results when applied to engineering problem.

In order to further comparing the effect of different discretization scheme on LES, here we run a series cases with the same TNS model (all using 6th order Padé filter) while the spatial discretization uses spectral method and different order of Padé schemes. The results are shown in Fig. 5.8 and Fig. 5.9. Similar to DNS, low order Padé discretization scheme leads energy to accumulate at high modes. Higher the order is, the result is more close to DNS. The spectral method is the best one. But different form DNS, low order (2nd order) scheme obtains reasonable result and does not cause divergence like DNS case in Fig. 5.5. It is because the TNS model removes the unphysical energy accumulated at high modes and thus dumps the discretization error.

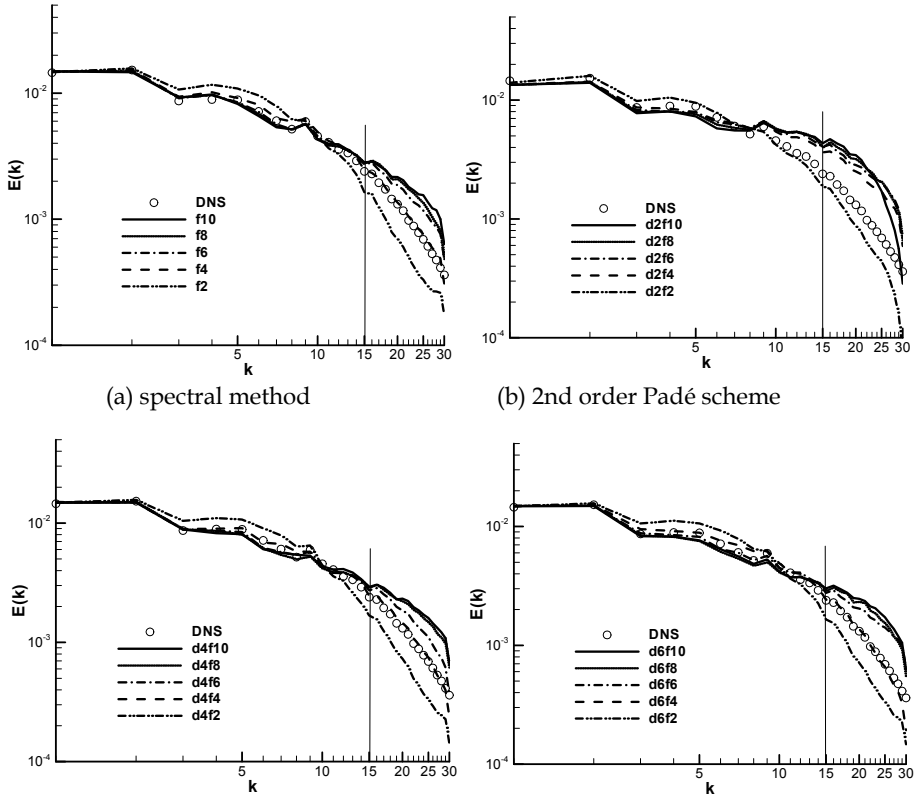

(a) spectral method (b) 2nd order Padé scheme

(c) 4th order Padé scheme (d) 6th order Padé scheme

Fig. 5.7. The final energy spectrum for LES using spectral method, different order Padé schemes and TNS models.

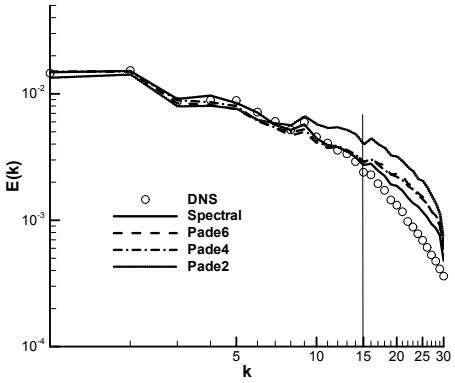

Fig. 5.8. The final energy spectrum for different discretization scheme with the same TNS model.

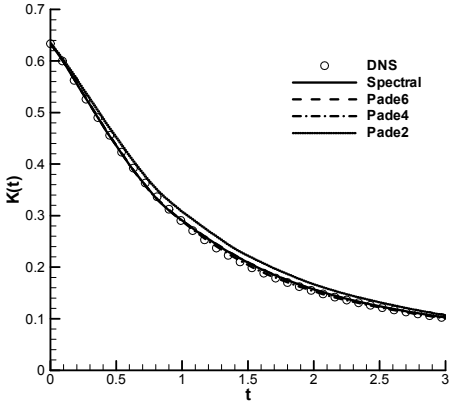

Fig. 5.9. The time evolution of total energy for different discretization scheme with the same TNS model.

Same to Fig. 5.6, we also try to investigate the effect of anti-aliasing method on the final results (only the case using 6th order Padé scheme, 6th TNS model is considered). The comparison is shown in Fig. 5.10. The aliasing error is still small. But for LES the energy at cut-off wavenumber is considerable large compared to DNS, the relative value of aliasing error increases.

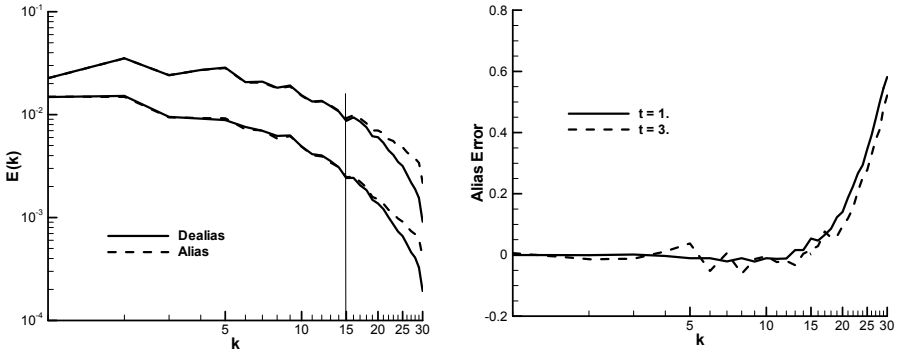

(a) (b)

Fig. 5.10. The aliasing error for LES using 6th Padé scheme and TNS model with 6th order filter.

6. Conclusion

In the past ten years significant progress has been made in the LES technology. LES has become one of the most promising and successful methodology available to solve the complex turbulent flows. However there are still some challenges before LES can be a mature tool to predict engineering problems, including reliable subgrid scale model, the choice of filter, near-wall treatment, numerical errors etc. And an accurate, fast and robust numerical algorithm for complex geometry is also needed. In this article, three key issues of

LES, namely the SGS models, the choice of filters and the effects of numerical errors, are investigated briefly.

The TNS approach is a simple and promising model. It actually is a DNS run with periodic processing of high modes. The basic assumption in TNS is that dynamics of small scales are strongly determined by the large eddies and the contribution of small scales to large scales are mostly contained within wavenumbers that are twice that of the cut-off wavenumber. By periodic removal of high mode energy using a filter, TNS provides necessary dissipation for small scales and thus avoids energy accumulation at high wavenumbers. It provides natural dissipation mechanism for low modes by nonlinear interactions between low modes and high modes at the cost of doubling the mesh. It can be expended to other flow easily because it does not have any empirical parameter.

The filtering operation plays a key role in TNS. It is responsible for removing the accumulated energy of the small scales at prescribed intervals. The filter type has direct effect on the final simulation results. Here a set of smooth filters and discrete filters are tested using TNS model. For the smooth filters, the physical filter is implemented in the physical space while it has similar property to the spectral filter at the same time. Also it keeps a part of the small-scale energy, which benefits the energy transfer. The Tophat and Gaussian filters are easy to implement but have serious undesirable effects on the large-scale energy. The discrete Padé filters exhibit advantages over the V-filters because the effect of adjacent points can be taken into account. The Padé filters can keep most of large-scale energy while maintaining sufficient amount of the small-scale energy at the same time. They show very good performance in all the runs, even better than the smooth physical filter. However the second order Padé filter still has effect on the large scales and the high order ones tend to keep too much small-scale energy, both of them may decrease the performance of TNS. The V-filters can be easily implemented to any specified order. However, high asymmetric filters should be avoided because they introduce too much nonphysical energy at high modes. The second order symmetric V-filter is actually a discrete version of the Tophat filter. It has the same problem as the smooth one, i.e., removing too much large-scale energy. When the smooth physical filter idea is applied to the V-filters, the results for the low order V-filters are improved significantly, but it is not necessary for high order V-filters. Note that the filter type should be adjusted according to the SGS model. So for LES with other SGS models, the effect of filters may be different.

The effects of numerical errors on LES are investigated briefly here, including discretization error, alias errors as well as SGS model error. As for DNS, no matter using spectral method or Padé compact scheme, the aliasing error can be well controlled. The final result is more affected by the truncation error of discretization scheme. High order scheme is preferred. Low order scheme is not suitable in some case. For example in our simulation, 2nd order discretization scheme leads energy to accumulate at high modes quickly and causes the solution unstable. As for LES, the interaction between numerical error and SGS model is complicated. Different model, such as TNS with different order filtering, can have different results. Low order filter brings in too much dissipation which is not a suitable property for LES; while the dissipation provided by high order filter is too small which also decreases the performance of TNS model. High order discretization schemes (4th order Padé scheme and above) plus middle order filters (4th or 6th order) can obtain good results compared with DNS. A more advantage is that TNS model not only avoids the small scales energy accumulating, but also dumps the side effect of discretization and alias errors to the high modes because TNS model removes the high modes energy periodically by filtering. This

interaction between TNS model and numerical error benefits LES. So low order discretization scheme plus a more dissipative TNS model can get good enough result. In addition, the energy at cut-off wavenumber for LES is still relative large, so the effect of aliasing error increases. We have to admit that due to the time and our knowledge limitation, the study on the numerical error is not full enough. There are some excellent works by other researches available.

7. Acknowledgment

This research is supported by NSF China Grants No. 10502029, Hunan nature science found 10JJ3018 and the Science Fund of State Key Laboratory of Advanced Design and Manufacturing for Vehicle Body 31075013. I am greatly grateful to Dr. Domaradzki and Dr. Song Fu for many useful discussing and advising on this research.

8. References

Bertero, M and Boccacci P (1998). *Inverse Problems in Imaging*. Institute of Physics Publishing. ISBN 0750304359. Bristol, United Kingdom

Bouffanais, B. (2010). Advances and challenges of applied large-eddy simulation. *Computers & Fluids*, vol. 39, (December 2010), pp.735–738

Chollet, J. and Leiseur, M. (1981) Parameterization of small scales of three dimensional isotropic turbulence utilizing spectral closures. *J. Atmos. Sci.* Vol.38, (1981), pp.2747-2757

Chow, F. Moin P. (2003). A further study of numerical errors in large-eddy simulations[J]. *Journal of Computational Physics*, Vol.184, (2003), pp.366–380

Dahlstrom S and Davidson L. (2003). Large Eddy Simulation Applied to a High Reynolds Flow around an Airfoil close to stall. *AIAA paper 2003–0776*

De Stefano G. Vasilyev O. (2002). Sharp cutoff versus smooth filtering in large eddy simulation. *Physics of fluids*, Vol.14, No.1, (2002), pp.362-369

Domaradzki, J. Loh, K. Yee, P. (2002). Large eddy simulation using the subgrid-scale estimation model and truncated Navier-Stokes dynamics. *Theor. Comput. Fluid Dyn.*, Vol.15, No.6, (2002), pp.421-450

Domaradzki, J. Rogallo, R. (1990). Local energy transfer and nonlocal interactions in homogeneous, isotropic turbulence. *Phys. Fluids A*, Vol.2, (1990), pp.413.

Domaradzki, J. Saiki, E. (1997). A subgrid-scale model based on the estimation of unresolved scales of turbulence. *Phys. Fluids*, Vol.9, (1997), pp.2148

Fauconnier, D. Langhe, C. Dick E. (2009). A family of dynamic finite difference schemes for large-eddy simulation. *Journal of Computational Physics*, Vol.228, (2009), pp.1830–1861

Fröhlich J. Rodi W. (2001). Introduction to Large Eddy Simulation of Turbulent Flows, In: *Closure Strategies for Turbulent and Transitional Flows*, Launder and Sandham. pp.267-298, Cambridge University Press, ISBN 9780521792080, UK

Georgiadis, N. (2008). Large-eddy simulation - Current capabilities and areas of needed research. *Progress in Aerospace Sciences*, vol.44, (2008), pp.379–380

Germano, M. Piomelli, U. Moin, P. Cabot, W. (1991). A dynamic sub-grid-scale eddy viscosity model. *Phys. Fluids A*, Vol.3, No.7, (1991), pp.1760-765.

Ghosal, S. (1996). An analysis of numerical errors in large-eddy simulations of turbulence. *J. Comput. Phys*. Vol.125, (1996), pp.187–206

Hartel, C. Kleiser, L. Unger F. Friedrich, R. (1994). Subgrid-scale energy transfer in the near-wall region of turbulent flows. *Phys. Fluids*, Vol.6, (1994), pp.3130

He, G. Wang, M. Lele, S. (2004). On the computation of space-time correlations in decaying isotropic turbulence. *Physics of Fluids*, 2004, Vol.14, No.11, (2004), pp.3859-3867

Horiuti, K. (1999). Transformation properties of subgrid-scale models in a frame of reference undergoing rotation. *Submitted to the J. Fluid Mech.* (1999).

Kitoh, K. Oshima, N. Yamamoto, M. etc. (2009). A CFD Approach via Large Eddy Simulation to the Flow Field with Complex Geometrical Configurations: A Study Case of Vehicle Underbody Flows. *SAE 2009-01-0332*

Krajnovic, S. Davidson L. (2005). Flow Around a Simplified Car, Part 1: LES. *Journal of Fluids Engineering, Transactions of the ASME*, vol.127, (2005), pp.907 -918

Kravchenko, A. Moin, P. (1997). On the effect of numerical errors in large eddy simulations of turbulent flows. *Journal of Computational Physics*, Vol.131, No.2, (1997), pp.310–322

Lele, S. (1992). Compact finite difference schemes with spectral-like resolution. *Journal of Computational Physics*, Vol.103, (1992), No.1, (1992), pp.16-42

Leonard A. (1974). Energy cascade in large eddy simulations of turbulent fluid flows. *Adv. Geophys. A*, Vol.18, (1974), pp.237-248

Lesieur, M. (1990). *Turbulence in Fluids* (2nd Edition). Kluwer Academic Publishers. ISBN 978-1-4020-6434-0. Springer, The Netherlands.

Lilly, D. (1992). A proposed modification of the Germano subgrid-scale closure method. *Phys. Fluids A*, Vol.4, (1992), pp.633

Lilly, D. (1996). On the application of the eddy viscosity concept in the inertial subrange of turbulence. *NCAR manuscript 123*, (1996), NCAR, Boulder, CO.

Lund, T. (1997). On the use of discrete filters for large eddy simulation, *Center for Turbulence Research*, Annual Research Brief, (1997), pp.83

Lund, T. (2003). The Use of Explicit Filters in Large Eddy Simulation. *Computers and Mathematics with Applications*, Vol.46, (2003), pp.603-616

Mahesh, K. Constantinescu, G. Moin, P (2004). A numerical method for large-eddy simulation in complex geometries. *Journal of Computational Physics*, vol.197, (January 2004), pp.215–240

Mary I. and Sagaut P. (2001). Large Eddy Simulation of Flow Around an Airfoil. *AIAA paper 2001-2559*

Mathew, J. (2010). Large Eddy Simulation. *Defence Science Journal*, Vol.60, No.6, (November 2010), pp 598-605

Mathew, J. Lechner, R. Foysi, H. Sesterhenn, J. Friedrich, R. (2003) An explicit filtering method for large eddy simulation of compressible flows. *Physics of Fluids*, Vol.15, No.8, (2003), pp.2279-2289

McCallen, R. *et al.* (2006). DOE's Effort to Reduce Truck Aerodynamic Drag through Joint Experiments and Computations. (2006) DOE 21CTP-0003

Mellen, C. Fröhlich, J. Rodi, W. (2003). Lessons from LESFOIL project on large-eddy simulation of flow around an airforl. *AIAA Journal*, vol.41, No.4, (2003), pp.573-581

Minguez, M. Pasquetti R. Serre. E. (2008). High-order large-eddy simulation of flow over the 'Ahmed body' car model. *Physics of Fluids*, Vol.20, No.9, (2008), pp.95-101

Moin, P. (2002). Advances in large eddy simulation methodology for complex flows. *International Journal of Heat and Fluid Flow*, vol.23, (2002), pp.710–720

Park, N. Mahesh K. (2007). Analysis of numerical errors in large eddy simulation using statistical closure theory. *J. Comput. Phys*. Vol.222, (2007), pp.194–216.

Piomelli, U. (1999). Large-Eddy simulation: achievements and challenges. *Progress in Aerospace Science*. Vol.35, (1999), pp.335

Piomelli, U. Moin, P. Ferziger, J. (1988). Model consistency in large eddy simulation of turbulent channel flow. *Phys. Fluids*, Vol.31, (1988), pp.1884.

Pope, S. (2000). *Turbulent Flows*. Cambridge University Press. ISBN 0521591252. Cambridge, United Kingdom

Rodi, W. (2006). DNS and LES of some engineering flows. *Fluid Dynamics Research*, vol.38, (2006), pp.145-173

Rogallo, R. (1981). Numerical experiments in homogeneous turbulence. *NASA Tech. Memo*. 81835, 1981

Sagaut, P. (2006). *Large-eddy simulation for incompressible flows – an introduction* (3rd Edition). Springer. ISBN 978-3-540-26344-9. Berlin, German

Smagorinsky, J. (1963) General circulation experiments with the primitive equations I: The basic experiment. *Monthly Weather Review.* Vol.91, No.3, (1963), pp.99-165

Spalart, P. (2000). Strategies for turbulence modelling and simulations. *International Journal of Heat and Fluid Flow*. Vol.21, (2000), pp.252-263

Stolz, S. Adams, N. (1999). An approximate deconvolution procedure for large- eddy simulation. *Phys. Fluids*, Vol.11, (1999), pp.1699-701.

Tsubokura, M. Kobayashi, T. Nakashima, T. *et al.* (2009). Computational visualization of unsteady flow around vehicles using high performance computing. *Computers & Fluids*, Vol.38, (2009), pp.981–990

Vasilyev O. Lund, T. and Moin P. (1998). A general class of commutative filters for LES in complex geometries. *Journal of Computational Physics*, Vol.146, (1998), pp.82-104

Visbal M. Gaitonde D. (2002). On the use of higher-order finite-difference schemes on curvilinear and deforming meshes. *Journal of Computational Physics,* Vol.181, (2002), pp.155-185

Yang, X. Domaradzki J. (2004) Large eddy simulations of decaying rotating turbulence. *Physics of Fluids*, Vol.16, No.11, (2004), pp.4088-4104

Yang, X. Fu S. (2008). Study of numerical errors in direct numerical simulation and large eddy simulation. *Applied Mathematics and Mechanics*. Vol.29, No.7, (2008), pp.871-880

Zhou, Y. (1993). Interacting scales and energy transfer in isotropic turbulence. *Phys. Fluids A*, Vol.5, (1993), pp.2511

Computational Simulations and Applications

Edited by Dr. Jianping Zhu

ISBN 978-953-307-430-6
Hard cover, 560 pages
Publisher InTech
Published online 26, October, 2011
Published in print edition October, 2011

The purpose of this book is to introduce researchers and graduate students to a broad range of applications of computational simulations, with a particular emphasis on those involving computational fluid dynamics (CFD) simulations. The book is divided into three parts: Part I covers some basic research topics and development in numerical algorithms for CFD simulations, including Reynolds stress transport modeling, central difference schemes for convection-diffusion equations, and flow simulations involving simple geometries such as a flat plate or a vertical channel. Part II covers a variety of important applications in which CFD simulations play a crucial role, including combustion process and automobile engine design, fluid heat exchange, airborne contaminant dispersion over buildings and atmospheric flow around a re-entry capsule, gas-solid two phase flow in long pipes, free surface flow around a ship hull, and hydrodynamic analysis of electrochemical cells. Part III covers applications of non-CFD based computational simulations, including atmospheric optical communications, climate system simulations, porous media flow, combustion, solidification, and sound field simulations for optimal acoustic effects.

InTech Europe
University Campus STeP Ri
Slavka Krautzeka 83/A
51000 Rijeka, Croatia
Phone: +385 (51) 770 447
Fax: +385 (51) 686 166
www.intechopen.com

InTech China
Unit 405, Office Block, Hotel Equatorial Shanghai
No.65, Yan An Road (West), Shanghai, 200040, China
中国上海市延安西路65号上海国际贵都大饭店办公楼405单元
Phone: +86-21-62489820
Fax: +86-21-62489821